Loading Capacity and Dilute Nitric Acid Rinse of Diglocolamide Resin for the Recovery of Transplutonium and Rare Earth Elements from Mark-18A Targets

Matthew S. Mills* and Samuel Uba

Savannah River National Laboratory, Aiken, South Carolina 29898, United States

*Email: Matthew.Mills@srnl.doe.gov

SRNL-STI-2024-00498

Loading Capacity and Dilute Nitric Acid Rinse of Diglocolamide Resin for the Recovery of Transplutonium and Rare Earth Elements from Mark-18A Targets

ABSTRACT

N,N,N′,N′-tetraoctyldiglycolamide (TODGA) as a resin ("DGA resin") produced by Eichrom Technologies will be used by Savannah River National Laboratory for the indiscriminate extraction of trivalent actinides and rare earth elements with the intent of recovering Cm and Am from dissolved irradiated ^{242}Pu Mark-18A targets in 7 to 9 M nitric acid. The extracted constituents will be recovered as an oxide by direct thermal decomposition of the loaded resin followed by calcination of the resultant residue. The characteristics of DGA resin with non-radiological feed simulant representative of the anticipated feed in the Mark-18A process, with Sm and Nd as surrogates for Cm and Am, respectively, including breakthrough point and saturation capacity were evaluated in this work. Additionally, this work examined the losses from the loaded resin by rinsing the resin bed with dilute acid to reduce the nitrate concentration in the resin bed prior to thermal decomposition operations to improve the safety posture of the process. A resin loading profile was developed, and the resin was determined to have a trivalent metal saturation capacity of 74 μmol/mL resin under the experimental conditions evaluated. Following a wash of the loaded resin bed with fresh 8 M HNO_3, the trivalent metals retained was reduced to 68 μmol/mL resin, which represents the practical capacity of the resin for the Mark-18A process. Lighter lanthanides breakthrough the resin well before the saturation capacity is reached. Rinsing the saturated resin bed with 0.26 M HNO_3 was found to result in a rapid reduction in retention of rare earth elements by the resin. After 2.8 bed volumes of dilute acid rinse, the mean resin bed free acid concentration was reduced to 0.28 M and 3.1 bed volumes of dilute acid rinse resulted in a reduction of the cumulative rare earth element retention to 52 μmol/mL of resin.

Keywords: Transplutonium separations; rare earth element separations; resin calcination.

INTRODUCTION

Savannah River National Laboratory (SRNL) has developed a separations flowsheet for the recovery of valuable elements contained in irradiated ^{242}Pu Mark-18A (Mk-18A) targets. These targets originally contained up to nominally 120 g of >98 atom percent ^{242}Pu and were irradiated in the Savannah River Site's K-Reactor for about ten years under a neutron flux of up to 10^{15} neutrons cm^{-2} s^{-1}. The original purpose of these targets was to produce heavy Cm (≥50% ^{246}Cm) as ^{252}Cf feedstock but the present interest in the targets is primarily their rich amount ^{244}Pu, the longest-live isotope of Pu.[1] Curium must also be recovered from the targets to comply with SRNL's high-activity residue requirements and has value for the Department of Energy's isotope production program. Additionally, the Mk-18A targets contain ^{243}Am, the longest-lived isotope of Am, which is desirable for research purposes.

The Mk-18A separations flowsheet includes a caustic dissolution of the target's aluminum cladding. The majority of the target material, including the actinides, rare earth elements (REEs), and other fission products, are insoluble in the caustic media. The undissolved solids are filtered and dissolved in nitric acid (HNO_3) at or near boiling. The resultant solution is adjusted to 7-9 M HNO_3, and Pu is recovered from the solution by anion exchange via Reillex HPQ resin packed in a continuous flow column. The Reillex resin has a high affinity for tetravalent actinides (e.g., Pu(IV)), which load onto the resin as a hexanitrato complex from a high nitrate solution matrix, rejecting the trivalent Cm, Am, and REEs along with the remaining fission products to the raffinate.[2-4]

Curium and Am will be separated from the anion exchange raffinate via *N,N,N',N'*-tetra-n-octyldiglycolamide (TODGA) resin, which is produced as a solid resin by Eichrom Technologies Inc. under the trade name of DGA Resin. The resin is composed of 40% w/w TODGA physisorbed onto a polymethyl methacrylate (PMMA) support structure, representing the balance of the resin mass. TODGA extracts trivalent actinides and REEs from nitric acid solutions and generally has a low affinity for non-REE transition metals with some exceptions.[5-7] The final form of the Cm and Am material will be an oxide. Both the TODGA and PMMA components of the resin are composed of only C, H, O, and N (CHON) atoms, and are thus completely incinerable.[8, 9] This property is leveraged to convert these metals from nitrate complexes sorbed to DGA resin to oxides via a two-step process in which the loaded resin is dried and thermally decomposed (i.e., reduced in both mass and volume) in the same process column in which it is loaded followed by calcination of the resultant residue.[10] The decomposition process occurs under argon while the resultant residue is calcined in air.

The baseline flowsheet was to perform the thermal decomposition process with the resin under the same 7 to 9 M HNO_3 conditions from which it was loaded followed by washing with fresh acid of similar concentration to displace the feed. However, there were concerns about performing the resin thermal

decomposition process of the organic resin in the presence of this high concentration of nitric acid, an oxidizer, potentially resulting in uncontrolled combustion of the resin. As a result, it was requested that this 7 to 9 M HNO_3 be displaced from the resin bed prior to furnace operations.

While it is desirable to reduce the amount and concentration of nitric acid in the resin bed prior to furnace operations, it was acknowledged that this could result in product losses. Eichrom's data indicate that the distribution coefficient for Am(III) decreases with decreasing nitric acid concentration.[7] Distribution coefficients reported for the extraction of Am and Cm using dissolved TODGA in organic liquids from a nitric acid solution indicate that Cm has a higher affinity for TODGA than Am and the distribution coefficient trends are similar and proportional to the nitric acid concentration.[11, 12] However, past SRNL experience is that eluting from DGA resin with dilute nitric acid (e.g., pH 2) is challenging.[13] This is believed to be due to the difficulty in completely displacing the nitric acid to levels less than 0.1 M. Furthermore, Eichrom recommends stripping the resin with dilute hydrochloric acid solutions rather than nitric acid, indicating the inefficiency of eluting with dilute nitric acid.

The purpose of this study was to quantify potential losses from the displacement of the 7 to 9 M HNO_3 from the resin bed prior to thermal decomposition furnace operations. Additionally, process knowledge has significantly developed since the last Mark-18A DGA study.[6] A loading profile was characterized with a more representative feed simulant and loading conditions than was utilized in previous work.

EXPERIMENTAL

I-grade DGA Resin – Normal of 300 – 840 μm bead size obtained from Eichrom Technologies was used for this study. The simulant was prepared by dissolving reagent grade nitrate salts obtained from Sigma-Aldrich in deionized water including $Fe(NO_3)_3•9H_2O$, $Cu(NO_3)_2•3H_2O$, $Sr(NO_3)_2$, $Y(NO_3)_3•6H_2O$, $La(NO_3)_3•6H_2O$, $Ce(NO_3)_3•6H_2O$, $Pr(NO_3)_3•6H_2O$, $Nd(NO_3)_3•6H_2O$, $Sm(NO_3)_3•6H_2O$, $Eu(NO_3)_3•5H_2O$, $Gd(NO_3)_3•6H_2O$, $Tb(NO_3)_3•6H_2O$, $Dy(NO_3)_3•xH_2O$, and $Ho(NO_3)_3•5H_2O$. Solutions of various HNO_3 concentrations were prepared by diluting ACS grade 68-70% w/w HNO_3, obtained from Thermo Fisher Scientific, in deionized water.

The resin was prepared for the experiment by wetting 15.0616 g (34 mL) of dry DGA resin as received in 98.8 mL of 8 M HNO_3 for several hours, filtering the resin, and rewetting in 98.2 mL of 0.35 M HNO_3 for several days. This resin slurry was then packed in a 1.5 × 30 cm Econo-Column Bio-Rad chromatography column, taking care the ensure that there were no gas bubbles in the resin bed, and the resin bed was topped with a glass frit. Support at the top of the resin bed is necessary as DGA resin is buoyant in 8 M HNO_3 but not 0.35 M HNO_3. The height of settled resin in the column was measured to be 24.2 cm from the 0.35 M HNO_3 slurry, providing a bed volume (BV) of 42.8 mL based on a column inner-

diameter of 1.5-cm. The initial height of the resin bed was marked on the glass column, and it was not observed to vary during the experiment or for months thereafter. During this work, it was observed the DGA resin swells upon hydration and swelling has been observed to be proportional to HNO_3 concentration. Therefore, it is important to contact the resin with the highest anticipated concentration of HNO_3 to which it is expected to be exposed during processing, prior to packing a column.

A representative simulant of the anticipated Mk-18A process DGA feed was prepared. Samarium and Nd were used as surrogates for Cm and Am, respectively, based on their similar distribution coefficient profiles for liquid DGA in solvent extraction systems.[11, 12] Both Sm and Nd are present in the Mk-18A targets. The simulant Sm and Nd concentrations were increased relative to the anticipated concentrations of these species to represent the sum of Sm and Cm and the sum of Nd and Am concentrations, respectively, on a mole basis. The feed was analyzed for metals by inductively coupled plasma mass spectrometry (ICP-MS) and for free acid by acid-base titration. All ICP-MS and free acid titration values for this work are reported with relative standard deviation (RSD) uncertainties of up to 10% and 5%, respectively. The composition of the feed simulant is provided in Table 1.

Table 1. Composition of DGA feed simulant.

Component	Concentration
Fe (μM)	4.69×10^{3}
Cu (μM)	4.03×10^{2}
Sr (μM)	5.74×10^{1}
Y (μM)	4.86×10^{1}
La (μM)	2.20×10^{2}
Ce (μM)	6.58×10^{2}
Pr (μM)	1.62×10^{2}
Nd[a] (μM)	1.17×10^{3}
Sm[b] (μM)	8.23×10^{2}
Eu (μM)	1.78×10^{1}
Gd (μM)	3.49×10^{2}
Tb (μM)	2.28×10^{1}
Dy (μM)	1.69×10^{1}
Ho (μM)	6.51×10^{0}
Er[c] (μM)	4.68×10^{0}
Tm[c] (μM)	1.55×10^{-2}
Yb[c] (μM)	4.11×10^{-1}
Lu[c] (μM)	3.86×10^{-2}
Sum of REEs (μM)	3.52×10^{3}
HNO_3 (M)	7.51×10^{0}

a. 93.6 mol% represents Nd, 6.4 mol% represents Am.
b. 16.1 mol% represents Sm, 83.9 mol% represents Cm.
c. Not specifically added to simulant but identified by ICP-MS. Likely impurities in other REE nitrate salts.

Solutions were pumped to the packed column via a Masterflex C/L Microflex peristaltic pump. The raffinate from the column was plumbed to flow through a 90-mm custom SRNL design flow cell like that used in the Mk-18A process in the Shielded Cells Facility. Column effluents were collected in tared polyethylene bottles. A photo of the experimental configuration is provided in Figure 1.

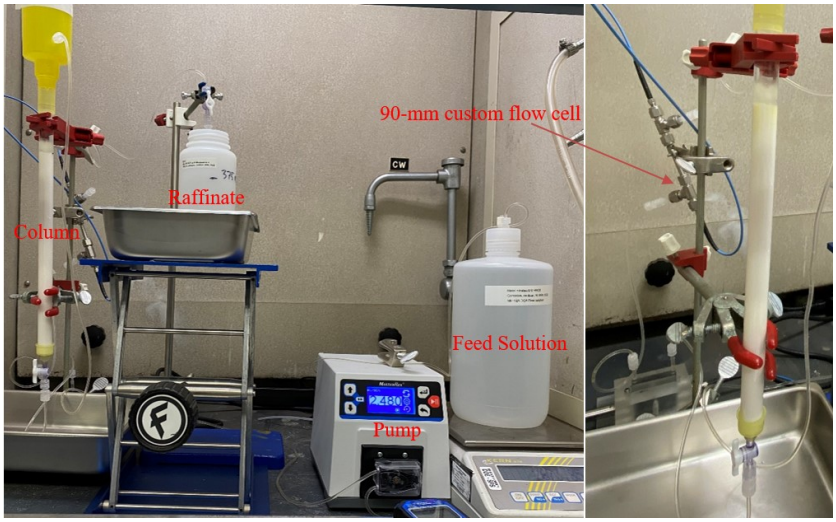

Figure 1. Experimental configuration.

The resin was conditioned with fresh 8 M HNO_3, loaded with the feed described in Table 1, washed with fresh 8 M HNO_3, and rinsed with 0.26 M HNO_3 with the following parameters. A resin rinse solution of 0.35 M HNO_3 was targeted as this solution is available in the process for the elution of the anion exchange resin. The difference in 0.26 and 0.35 M rinse acid concentrations is not expected to impact the conclusions of this work. The resin was intentionally saturated and loaded beyond the previously reported capacity to determine the bounding losses from a dilute acid rinse for conservatism. The column operating parameters for this experiment are provided in Table 2 below. The experiment was performed at ambient laboratory temperature (ca. 20 °C).

Table 2. Column operating parameters.

Step	Volume (BV)[a]	Average volumetric rate (BV h^{-1})	Average linear velocity (cm min^{-1})	Average REE flow rate (µmol cm^{-2} min^{-1})
Condition with 8 M HNO_3	4.50	6.26	2.52	-
Load	42.4	3.23	1.30	4.60
Wash with 8 M HNO_3	1.92	7.79	3.14	-
Rinse with 0.26 M HNO_3	3.24	6.66	2.68	-

[a] "BV" is bed volume and represents a volume of solution equivalent to the volume of the packed resin bed: 42.8 mL.

The effluent composites were weighed, sampled, and the density was measured. Samples of all effluent composite solutions, except the condition solution, were analyzed for metals by ICP-MS. Additionally, the dilute acid rinse composites were analyzed for free acid.

Spectrophotometric measurements were performed with a tungsten-halogen and xenon-arc flash lamp as light source, delivered via optical fiber cables to the custom designed flow cell. This flow cell was assembled from commercial-off-the-shelf (COTS) components and transmitted light intensities were measured using an Avantes Multichannel Spectrometer. Additional details of the optical system are provided in the Supplemental Information (SI). Real-time monitoring of the DGA column effluent was performed with a 90.01 ± 0.01 mm flow cell plumbed to promote a vertical up flow fluid direction. Transmitted light intensities of a collimated light beam from the flow cell were measured and interpreted by the Avantes spectrometer. The spectrometer was configured in a custom dual-beam diode array design and transmitted light intensities were measured by reference and sample detectors within an Avantes Multichannel Spectrometer. Light was integrated over 10 ms and 500 spectra were averaged by the spectrometer before passing the data to the control software to provide an average spectrum over approximately 5 second intervals. Absorbance values were calculated, and spectra were interpolated to a standardized set of wavelengths from 200 to 900 nm with 0.2 nm resolution using the instrument control software as described by Lascola, et al.[14]

RESULTS AND DISCUSSION

Loading

The average effluent composition, measured by ICP-MS, is shown in Figure 2. Detection of an element in the raffinate represents breakthrough from the resin. The measured composite concentration represents the average for each cut and is shown at the cumulative volumetric midpoint. Composite effluent compositions are provided in the SI.

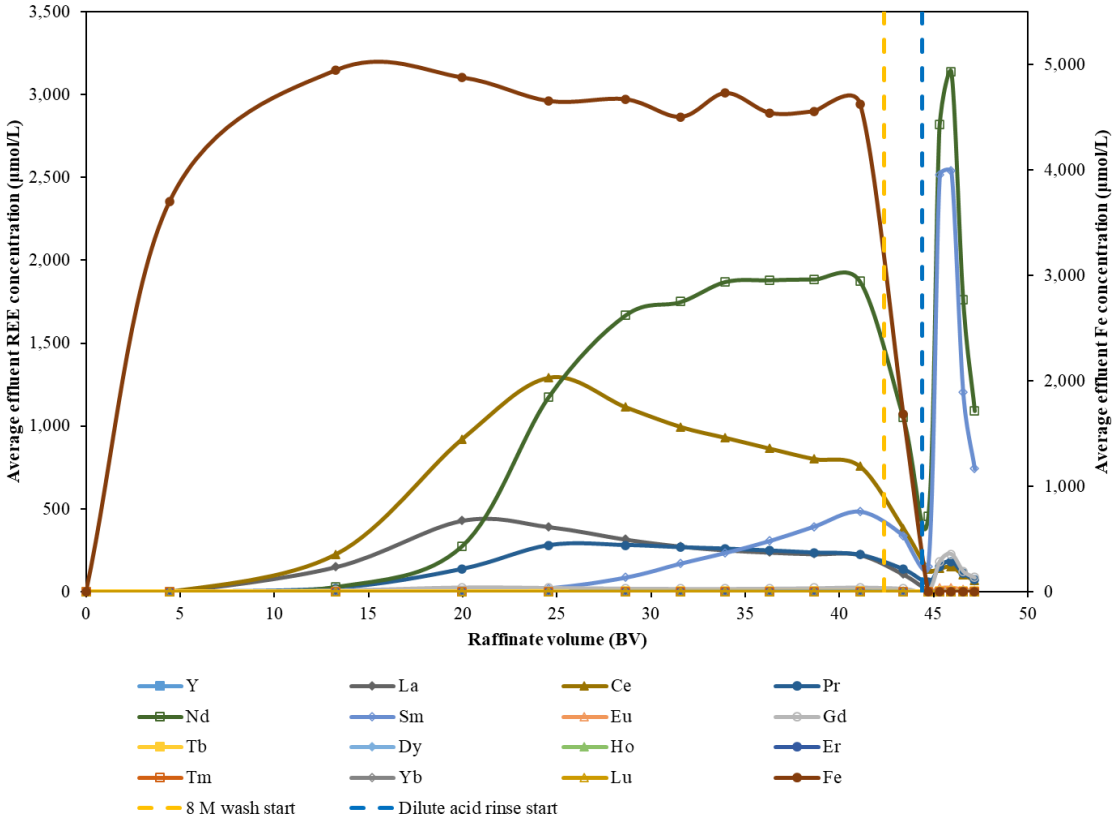

Figure 2. Average effluent composition.

The column loading profile, calculated based on the cumulative raffinate volume, measured feed concentrations, and measured effluent concentrations, is shown in Figure 3**Error! Reference source not found.**. The resin exhibited a REE capacity of up to 68 µmol/mL resin (~10 g of REEs/L resin) during loading with the feed simulant under these experimental conditions. This is determined by the maximum cumulative REE retention, which remains essentially constant once reached. Additionally, 6 µmol of Fe/mL resin was retained in the resin bed once the capacity was reached for an overall trivalent metal (M^{3+}) capacity of 74 µmol/mL resin during loading. Upon washing the resin bed with ~2 BV of fresh 8 M HNO_3, the REE and Fe retention were reduced to 64 and 4 µmol/mL resin, respectively, with an overall M^{3+} retention of 68 µmol/mL resin. The capacity reduction is due to the displacement of unextracted interstitial feed components and slight leaching of the saturated resin. Thus, this represents a practical capacity of the resin under the processing conditions of interest.

The resin capacity determined in this study is within the range of those reported in the literature. Horwitz et al. reported that the TODGA resin capacity is 77 µmol Eu/mL of resin bed in a slurry-packed column when loaded from a 0.0274 M Eu and 4.0 M HNO_3 feed.[7] The same paper states that the resin capacity is approximately 86 µmol Eu/mL of resin bed. Eichrom's website states that the DGA resin

functional capacity (i.e., with minimal breakthrough) is 7-8 mg Eu (46-53 µmol)/mL of resin.[15] The feed composition significantly influences retention. Distribution from the aqueous phase to TODGA increases with nitric acid concentration. A feed with a higher concentration of REEs and actinides is expected to have greater retention by the resin due to the increased driving force for mass transfer. For example, the Eu feed in Horwitz's study that resulted in a TODGA resin capacity of 77 µmol Eu/mL of resin bed is an order of magnitude higher than the REE concentration of the simulant for this study.[7]

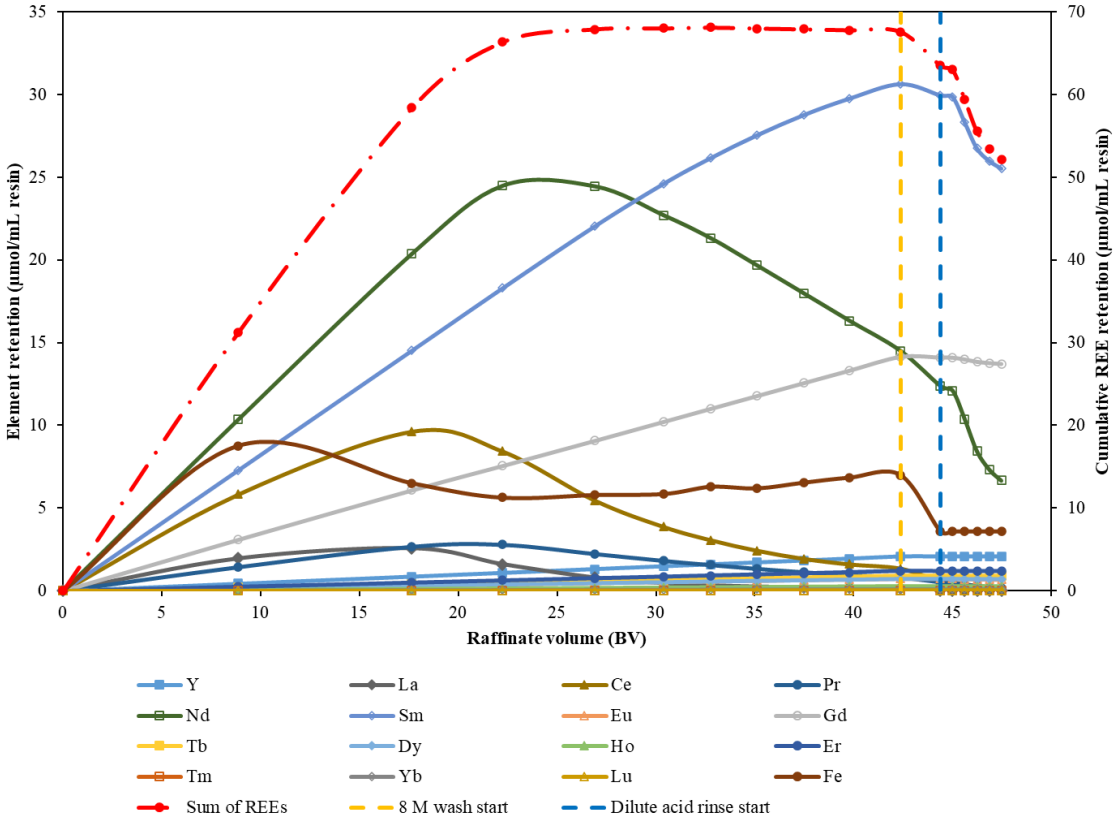

Figure 3. Resin loading profile.

Another metric for comparing the resin capacities is the stoichiometric capacity of TODGA. Horwitz et al. measured a TODGA to Eu mole ratio of 3.19:1 with the resin and concluded that this represents a TODGA to M^{3+} stoichiometry of 3:1.[7] This is consistent with the TODGA stoichiometry determined from a liquid-liquid extraction system with an aqueous solution of Nd and 3 M HNO_3.[16] Assuming the DGA Resin is 40 wt.% of 94% pure TODGA,[7] the TODGA to retained REE ratio measured in this work is 3.4:1 prior to the 8 M HNO_3 wash and 3.6:1 after the wash. Including Fe, the TODGA:M^{3+} ratio is 3.1:1 prior to the 8 M HNO_3 wash and 3.4:1 after the wash. Slight differences in resin capacities could be due to inefficiencies associated with the larger I-grade resin (300 – 840 µm) relative to the more common analytical DGA resin (50 - 100 µm) or the lower REE feed concentration of the feed in this study.

With this feed composition, Nd initially loads on the DGA resin at the highest concentration of all measured species followed by Fe, Sm, Ce, and Gd, respectively. As the resin sites approach saturation, lighter lanthanides are displaced in favor of heavier ones. Neodymium displacement by more strongly retained REEs (indicated by a hump in the loading profile in Figure 3**Error! Reference source not found.**) from the resin occurs as the resin approaches saturation with REEs. Neodymium displacement is preceded by the displacement of Ce and La. This is further illustrated in Figure 4. Iron is weakly retained by the resin, initially loading to 8.8 μmol/mL resin after 8.9 BV of feed. However, as more feed is processed through the column, Fe is partially displaced from the resin until a steady retention of nominally 6 μmol/mL resin is reached. The initial displacement of Fe is represented by an increase in the effluent concentration to above the feed concentration. Within 27 BV, the effluent Fe concentration settles to within ± 3% of the feed concentration. Iron is more concentrated than any other feed component by at least a factor of four and the Fe feed concentration is 33% higher than the sum of REEs. The high concentration of Fe in the feed likely results in a much higher retention than would be achieved with a feed concentration comparable to other components. The loading profile in Figure 3**Error! Reference source not found.** also demonstrates that there are significant losses from rinsing the saturated resin bed with dilute HNO_3, as indicated by decreased element and cumulative REE capacities and an increase in effluent concentrations. This is discussed in more detail below.

The percent retention of the REEs on the DGA resin with respect to the amount fed through the column is shown in Figure 4, which illustrates that 100% of the REEs are initially retained by the DGA resin up to at least 46% of the measured resin capacity in this study. However, once the resin is loaded to 86% capacity, the retention of low atomic number lanthanides is rapidly reduced, and breakthrough occurs. La through Nd successively breakthrough the resin in order of increasing atomic number between 8.8 and 17.6 BV of feed with cumulative REEs retained on the resin between 31 and 58 μmol (4.5 and 8.5 mg)/mL resin, respectively. This is consistent with data provided by Horwitz et al., which indicate that TODGA resin selectivity for lanthanides increases with atomic number. Their data also show that the relationship between resin selectivity and atomic number is logarithmic with more significant differences in selectivity at lower atomic numbers.[7] Horwitz et al.'s data were developed from batch contacts of resin with three stock solutions containing five to six REEs. The ratio of the elements to each other in these solutions is not clear. At atomic numbers greater than 60 (Nd), there are several differences in the trends observed in data developed in this study and that provided by Horwitz et al. For example, Sm (Z=62) is initially retained more than Gd (Z=64), Tb (Z=65), and Dy (Z=66). However, once the resin is saturated, the retention of Sm decreases significantly in favor of higher atomic number elements. Similarly, Eu (Z=63) has a higher retention throughout loading than Gd, Tb, and Dy. The initial strong retention of Sm over Gd, Tb, and Dy could be due to the significantly higher concentration of Sm in the feed. However, the feed concentrations

of Eu, Tb, and Dy are similar and the Gd feed concentration is an order of magnitude higher than Eu. Another difference in this data and that from the batch contacts in Horwitz et al.'s study is the retention of Y. Horwitz et al. found that the TODGA resin selectivity for Y is between Gd and Tb and the resin has a higher selectivity for lanthanides of atomic numbers greater than 65 than Y. The data developed in this study indicate that Y is the most strongly retained REE in the feed matrix with 100% retention during loading and minimal losses from resin washing and rinsing. Varying absorption and desorption kinetics of these species likely contributed to differences in element retentions in this study, with a dynamic flow column, and the batch contact data from Horwitz et al.

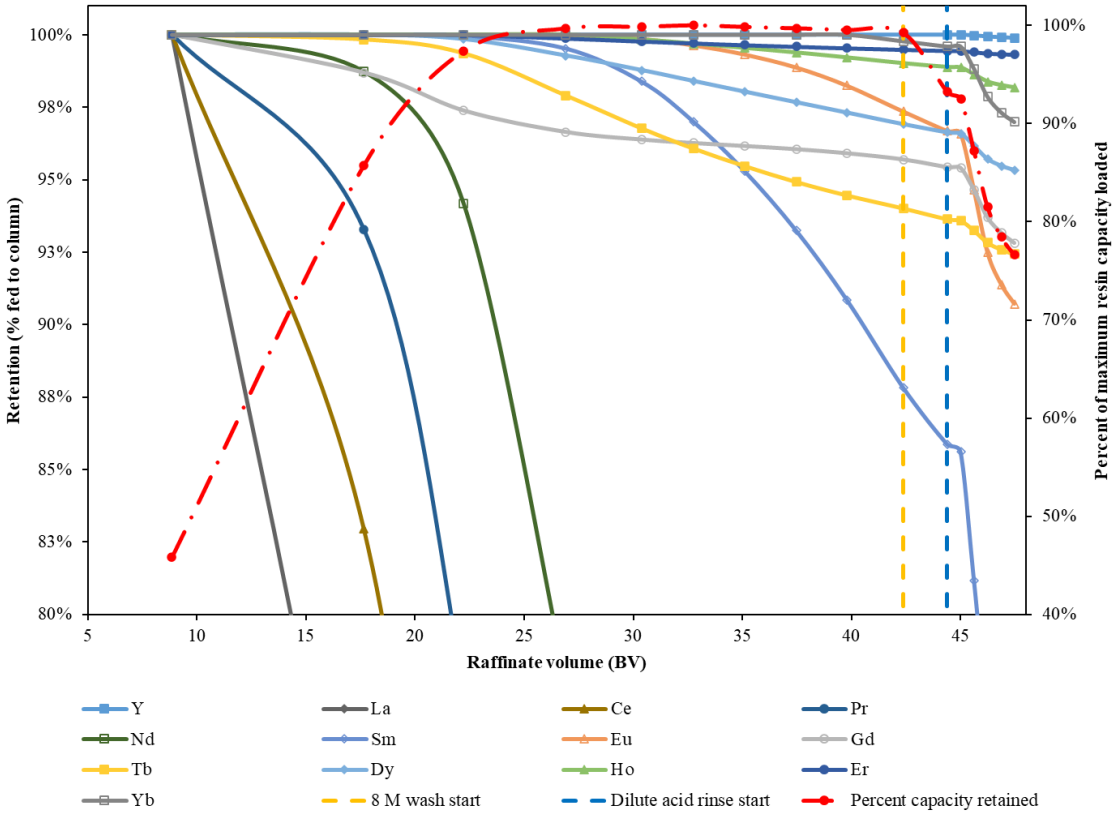

Figure 4. Element retention on DGA resin.

A previous SRNL DGA loading study reported that Nd breakthrough occurred with the resin loaded to 11 mg/mL resin with a similar feed matrix.[6] The Mk-18A process column was designed based on this metric, assuming 80% efficiency. The present study found that breakthrough occurs significantly earlier. In McCann et al.'s study, the 11 mg/mL resin breakthrough point was first identified with their "simulant 1", which was at least 7 times more concentrated than the anticipated feed concentration. They performed another experiment with "simulant 2", which was more dilute. The feed compositions between the experiment in the present study and the McCann simulant 2 experiment were generally similar (element

concentrations within ± 40%). Two notable exceptions are that McCann et al.'s simulant 2 Sm and Fe concentrations were 235% and 41% of the concentrations used in this study, respectively. McCann et al. stated that Nd began to breakthrough when the resin was loaded with simulant 2 to 11 mg REE, Am, and Zr/mL resin, as they predicted from results with a more concentrated simulant. However, there is ambiguity regarding the resin bed volume in the McCann experiment, used to calculate breakthrough capacity. In McCann et al.'s paper, the simulant 2 column is described as 2.2 × 20.3 cm with 77 mL of DGA Resin. However, the simulant 2 column is described as 2-cm ID packed to 20.3 cm with DGA Resin for 64 mL resin bed volume in the internal SRNL laboratory notebook for this work. If the loading of 11 mg REE, Am, and Zr/mL resin was calculated with a resin volume of 64 mL but the actual resin volume was 77 mL, then the loading at breakthrough would be 9.1 mg REE, Am, and Zr/mL resin, which is in reasonable agreement with the results of this study with 99% of Nd retained by the resin when loaded to 8.5 mg REE/mL resin.

If the breakthrough point for McCann et al.'s simulant 2 was correctly identified, the difference could be related, in part, to differences in flowrates and linear velocities in the present study and that used by McCann et al. The flowrates and linear velocities were 3.23 BV/h and 1.30 cm/min in this experiment and 2.6 BV/h and 0.89 cm/min in the McCann experiment, respectively. The loading rate for the 6.03 cm inner-diameter Mk-18A process DGA column is planned to be between 0.88 to 1.40 cm/min. Flowrate is inversely proportional to the residence time and linear velocity is inversely proportional to the time that the feed solution is in contact with a length of resin bed. The two parameters are similar, but both are important. Linear velocity is of particular importance because its inverse represents a kinetic limitation for cations to interact with discrete TODGA sites.

Figure 5 shows the effluent concentrations represented as a percent of the feed concentration at the volumetric midpoint for each cut. It illustrates the complex chromatographic interactions of these components with each other and DGA resin. The plot demonstrates that the effluent concentrations of lighter lanthanides, particularly La, Ce, Pr, and Nd, are initially non-detectable but that as more feed is processed, they evolve to significantly greater than the feed concentration. This is a result of these elements being displaced from the TODGA sites by more strongly retained components. By 42 BV of feed through the column, the effluent concentration of La was 102% of its feed concentration, indicating that it had essentially been completely displaced from the resin. Extrapolating the data, it is clear that Ce and Pr would follow suit with further processing. While Nd is also displaced from the TODGA sites by other components, its effluent concentration did not reach a peak followed by approaching the feed concentration like La, Ce, and Pr. Rather, the effluent concentration of Nd settles to 160% of the feed concentration between 35 to 42 BV of feed through the column. This indicates that while Nd is displaced by more strongly retained

components, Nd itself continued to displace La, Ce, and Pr. With further processing, the concentration of Nd would eventually approach 100% of the feed concentration as well.

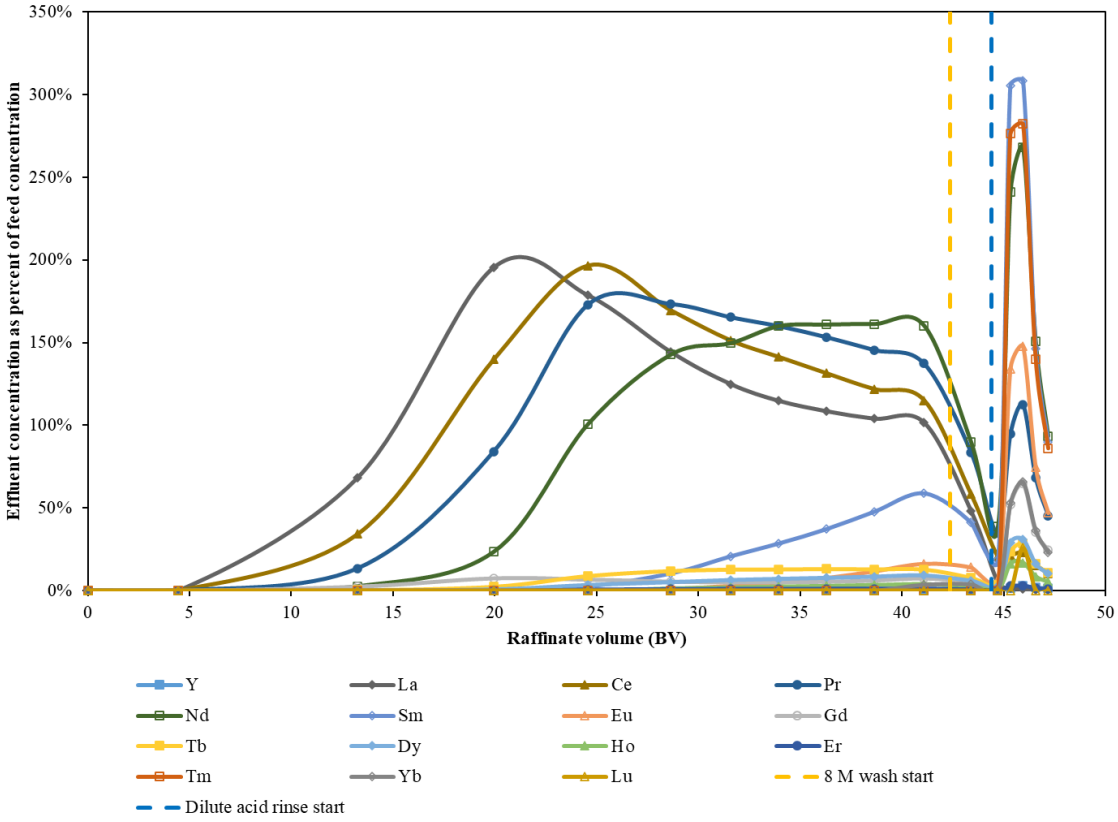

Figure 5. Effluent concentration as a percent of feed concentration.

Of particular interest in this study is the retention of Sm and Nd, which are present in the targets but also used as surrogates for Cm and Am, respectively. The volume of a quarter target batch of Mk-18A DGA feed is estimated to be equivalent to 22 BV of the nominally 750-mL DGA column. In this work, after 22.2 BV through the column, the resin was loaded with REEs to 66 µmol/mL resin (97% capacity), and 0% of Sm and 6% of Nd had broken through the resin bed. Curium and Am are represented as 83.9% and 6.4% of the Sm and Nd in the feed simulant, respectively. Thus, if these are perfect surrogates, 0% of Cm and 0.4% of Am are predicted to breakthrough with the richest quarter target during loading.

Figure 6 shows the real time effluent absorption spectra evolution during the loading and fresh 8 M HNO_3 wash phases of the experiment. The absorption band centered at ca. 393 nm is the most intense and represents Fe(III).[17] Iron is weakly retained by the resin and has no value to the program so the high absorbance is an inconvenient feature, but its development does provide some insight to early loading behavior. In particular, it can provide an indication of Fe displacement by more strongly retained actinides and REEs when the absorbance representing Fe at ca. 393 nm increases to greater than the absorbance in

the feed. At ~11 BV, absorption bands representing Nd developed at ca. 578 nm, 739 nm, and 791 nm.[6, 18, 19] As Nd continued to breakthrough the resin and the effluent concentration increased, the absorbance at these wavelengths grew significantly and further absorption bands representing Nd developed at ca. 510 nm, 523 nm, and 867 nm, by ~25 BV of feed. Shortly after beginning the fresh 8 M HNO_3 wash, the band centered at ca. 393 nm, representing Fe, was eliminated while the bands representing Nd approached a constant value. This is due to the displacement of interstitial feed from the resin bed. While the absorption band for Fe centered at ca. 393 nm was eliminated, absorption bands became distinguishable centered at ca. 370 nm and ca. 402 nm. These bands are attributed to Sm and were not distinguishable during loading, despite the increasing effluent Sm concentration as loading progressed.[18, 20] This is likely due to interference from the high absorption at ca. 393 nm representing Fe. Thus, Sm cannot be relied upon as an indicator of breakthrough for Cm in this matrix in the presence of Fe. The development of absorption bands representing Fe and Nd in the effluent during loading are consistent with average concentrations measured by ICP-MS, shown in Figure 2. The presence of the Nd bands in the raffinate provide a warning of forthcoming breakthrough of Cm or Am during actual Mk-18 processing. The most distinguishable Nd absorption occurs at ca. 578 nm. Light absorption at this wavelength should be monitored to predict potential breakthrough.

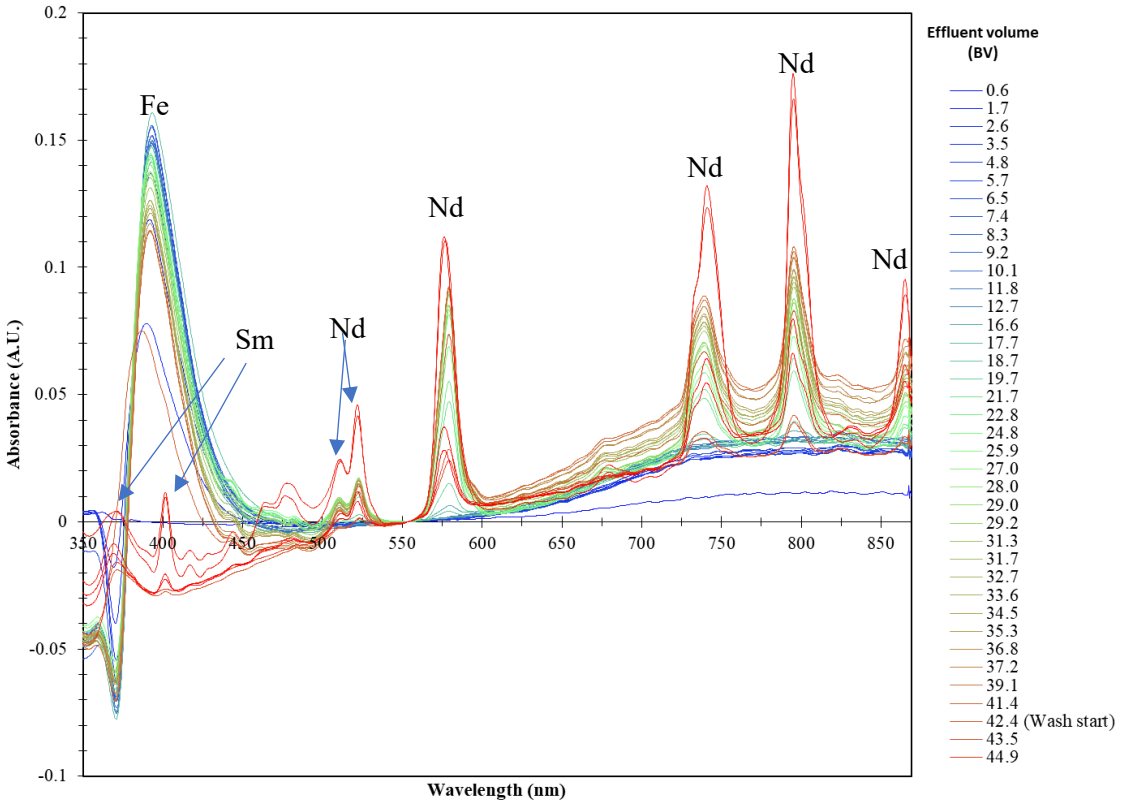

Figure 6. Absorption spectral evolution during loading and 8 M HNO_3 wash.

Dilute Acid Displacement

A primary objective of this study was to determine the losses from rinsing the loaded DGA resin bed with dilute nitric acid to reduce the column nitrate concentration prior to furnace operations. The resin was intentionally saturated to determine bounding losses. **Error! Reference source not found.**Figure 3 and Figure 4 demonstrate that there is a reduction in the retention of REEs to 77% of the maximum resin capacity obtained during loading from 3.1 BV of dilute acid rinse. The resin loading and acid profiles during the wash and rinse are provided in Figure 7. The mean free acid concentration was reduced from 7.5 M to 0.28 M after 2.8 BV of 0.26 M HNO_3 through the column. The cumulative REE retention on the resin was reduced to 52 µmol/mL of resin with 3.1 BV of total dilute acid rinse. Extrapolating the data, further but diminishing losses would be realized with additional rinsing of the resin bed.

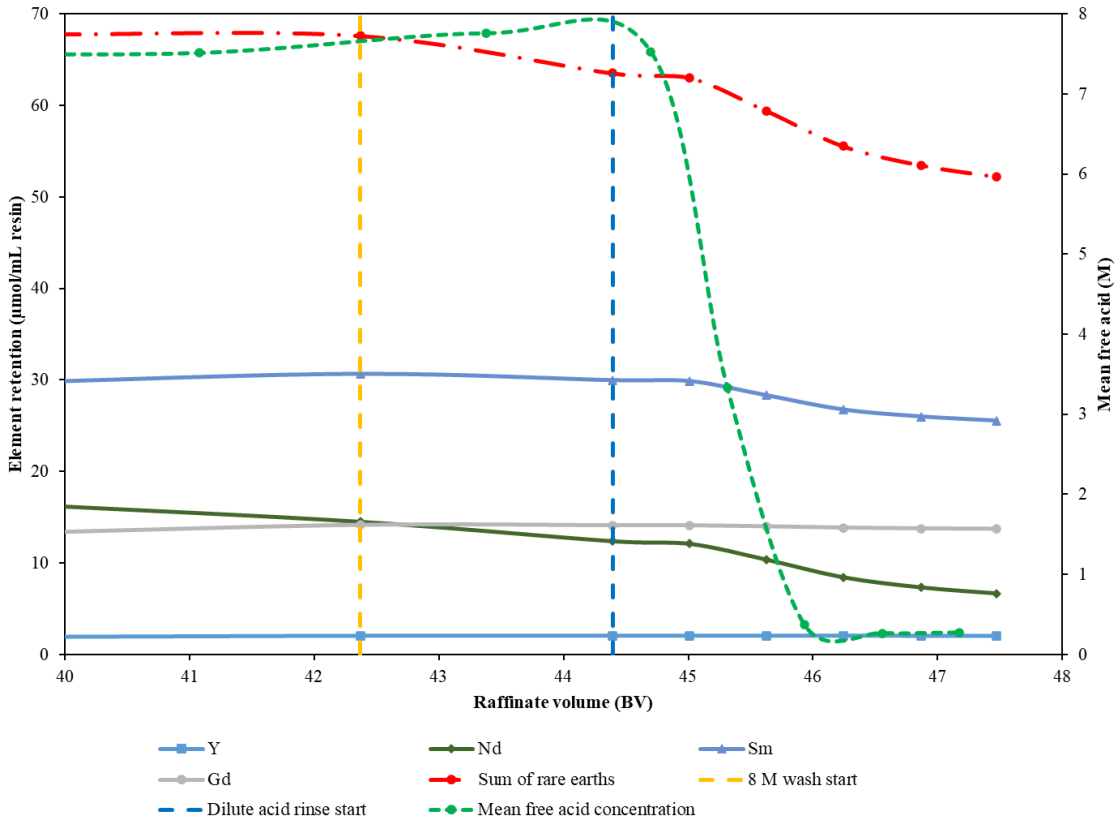

Figure 7. DGA retention and acid profile during resin bed 8 M HNO_3 wash and dilute HNO_3 rinse.

Figure 8**Error! Reference source not found.** shows REE retention on the resin during the dilute acid rinse relative to the pre-rinse loading (i.e., 0 BV corresponds to beginning of dilute acid rinse). It illustrates that Pr, Ce, and Nd experience the most significant reduction in retention by the resin during the dilute acid rinse. Lanthanum was already completely displaced from the resin by other REEs prior to the rinse. Similar to the loading behavior where these lower atomic number lanthanides were displaced from

the resin by heavier ones, they are also the most readily eluted from the resin under dilute acid conditions. There is less than a 3% reduction in the retention of Gd and heavier lanthanides from 3.1 BV of dilute acid rinse, except Tm, which is reduced by 11% of its pre-rinse concentration. Samarium, as a surrogate for Cm, exhibits a moderate reduction in retention of 15% with 3.1 BV of rinse.

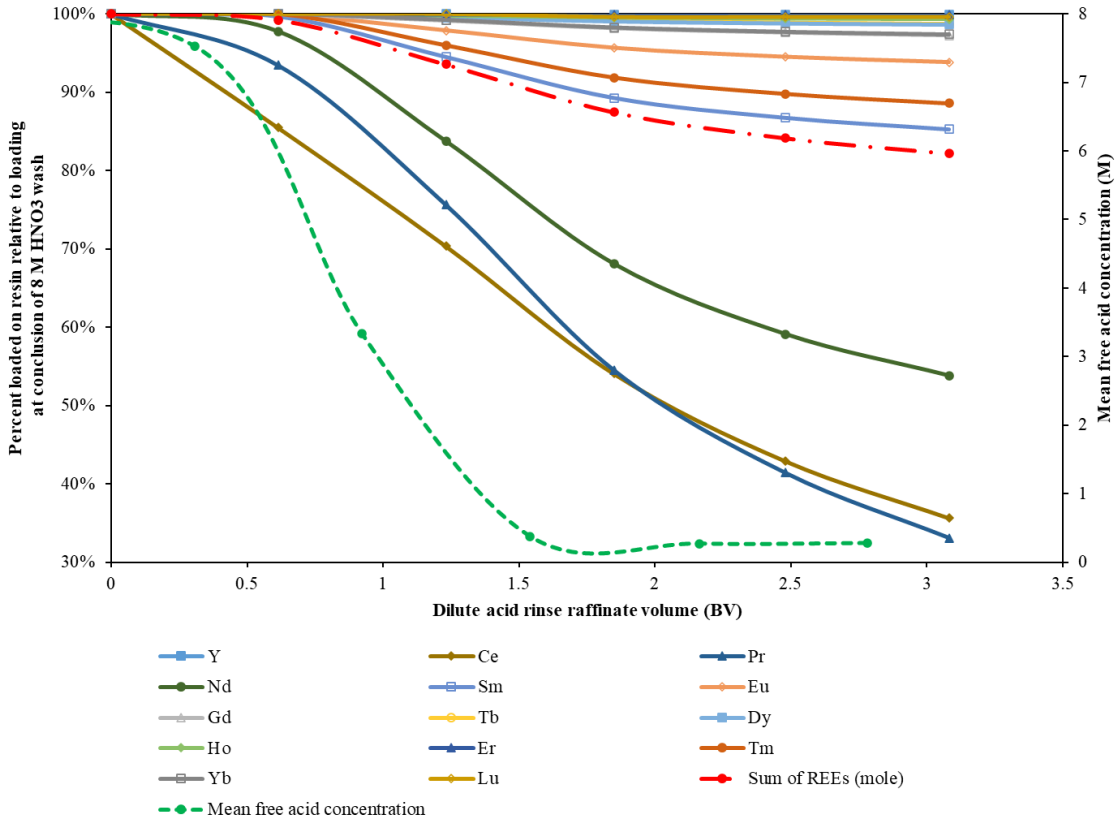

Figure 8. Resin retention from dilute acid rinse.

Losses of Cm and Am relative to the maximum amount contained in a quarter Mk-18A target are of particular interest to the program. Losses of no more than 5% of these values are targeted. The maximum amount of Cm and Am predicted in 25% of any target is 3.24 g and 0.33 g, respectively. The predicted losses of Cm and Am, assuming that they are represented by 83.9% and 6.4% of the Sm and Nd, respectively, relative to these maximum target values are provided in Figure 9. This analysis predicts Cm and Am losses to be significant based on measured Sm and Nd retention during this experiment, respectively. There is a substantial amount of Cm contained in the Mk-18A targets, which is represented by the majority of Sm in this experiment's simulant. There is far less Am contained in the targets but its surrogate, Nd, is retained less strongly than the Cm surrogate, Sm. Curium and Am losses are predicted to be 4.8% and 4.2% of the maximum amount contained in a quarter target from 1.2 BV of dilute acid rinse based on Sm and Nd losses in this experiment, respectively. This rinse volume is interpolated to provide a

resin bed HNO_3 concentration of 1.8 M. As a contingency to ensure no more than 5% of the Cm or Am is lost, 1 BV of rinse may be an appropriate target. This would result in predicted losses of 3.1% and 2.9% of the maximum amount of Cm and Am contained in a quarter target, respectively, and a resin bed HNO_3 concentration of 3.0 M. It is acknowledged that the desorption kinetics of Cm and Am under dynamic column flow conditions may differ from the desorption kinetics of their respective surrogates, Sm and Nd. Recycle of the column rinse effluent to the DGA feed tank is recommended so that this solution can be reprocessed with the next quarter target batch to further reduce overall process Am and Cm losses.

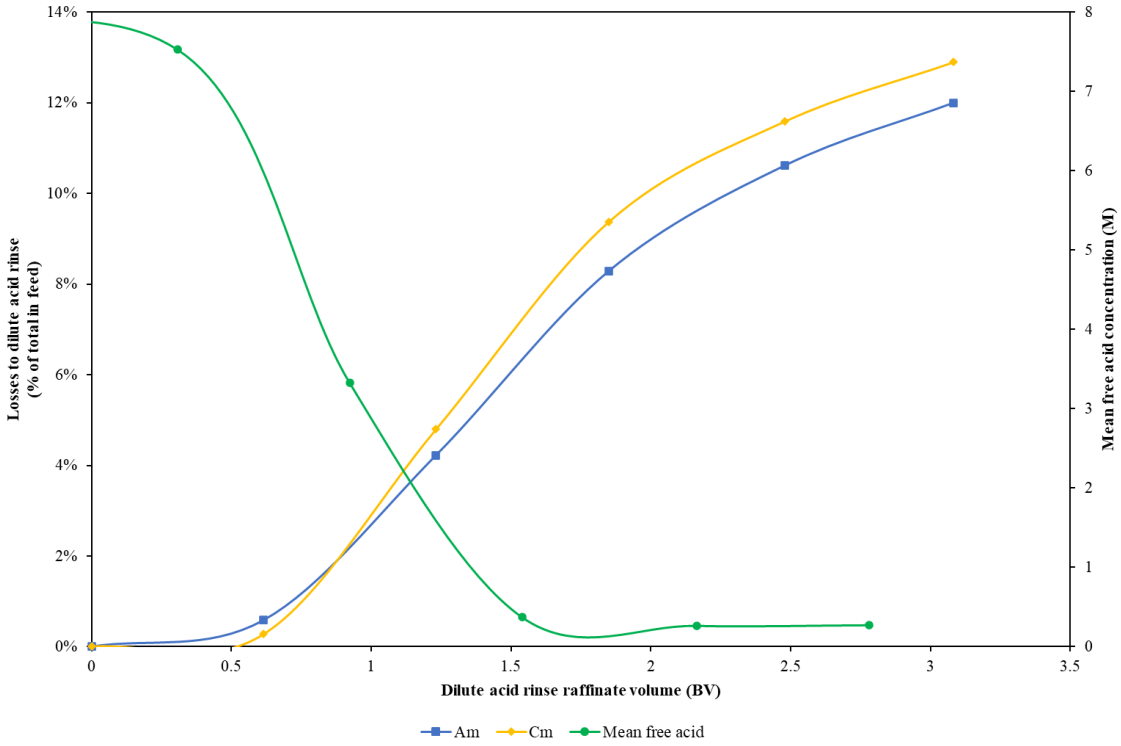

Figure 9. Predicted losses of Cm and Cm from dilute acid rinse.

In this experiment, the resin was loaded significantly beyond what is predicted for Shielded Cells operations. Thus, these loss predictions are conservative if Sm and Nd are conservative surrogates for Cm and Am. In this context, a conservative surrogate is one with less affinity for the extractant and would therefore desorb or be displaced from the resin more readily. Data provided by Zhu et al. for a 0.1 M TODGA/*n*-dodecane system and various concentrations of aqueous nitric acid indicate that the distribution coefficients for Am are similar to those for Nd but slightly higher, indicating Nd is a conservative surrogate.[5] This is consistent with data presented by Geist et al. for a 0.2 M TODGA/5% 1-octanol in TPH.[11] However, both Zhu and Geist show that the distribution coefficient for Sm is slightly higher than Cm across the range of nitric acid concentrations evaluated. Thus, in those solvent extraction systems, Sm has a stronger retention by TODGA than Cm. Extraction behavior on DGA Resin generally follows similar trends as

dissolved TODGA in a solvent extraction system.[7] Thus, Cm losses from the dilute acid rinse would likely be higher than predicted from Sm losses in this non-radiological experiment based on this data.

CONCLUSIONS

DGA Resin was loaded to saturation with a representative Mk-18A feed simulant. A loading profile was developed, and the resin was determined to have an M^{3+} saturation capacity of 74 µmol/mL resin, including 68 µmol (~10 mg) of REEs/mL resin and 6 µmol of Fe/mL resin. However, the post-washing M^{3+} capacity of 68 µmol/mL resin represents the practical capacity of the resin for this process. The saturation capacity determined in this work agrees with the literature, but the Nd breakthrough point with REE loading of ~58 µmol/mL resin is lower than reported in a previous study. Lighter lanthanides breakthrough the resin well before the saturation capacity is reached. Lanthanum through Nd breakthrough in order of increasing atomic number and Y was the strongest retained component by the resin. After 22.2 BV of feed through the column, similar to the amount estimated for the total process feed volume, the resin was loaded with REEs to 66 µmol/mL resin. At this point, 0% of Sm and 6% of Nd, surrogates for Cm and Am, respectively, broke through the resin bed.

Rinsing the saturated resin bed with 0.26 M HNO_3 was found to result in a rapid reduction of retention by the resin. After processing 2.8 BV of dilute acid rinse, the mean resin bed free acid concentration was reduced to 0.28 M and 3.1 BV of dilute acid rinse resulted in a reduction of the cumulative REE retention to 52 µmol/mL of resin. Like the loading behavior, lower atomic number lanthanides were the most readily desorbed components from the resin under dilute acid conditions. Estimating Cm and Am losses from the dilute acid rinse based on Sm and Nd losses, respectively, predicts that losses will be significant with excessive dilute acid rinse. Additionally, Sm may be more strongly retained by the resin than Cm, indicating that this approach could underpredict Cm losses.

Acknowledgments

The authors thank Eddie Kyser for his mentorship and technical insight during this work.

This work was produced by Battelle Savannah River Alliance, LLC under Contract No. 89303321CEM000080 with the U.S. Department of Energy. Publisher acknowledges the U.S. Government license to provide public access under the DOE Public Access Plan (http://energy.gov/downloads/doe-public-access-plan).

Disclosure Statement

The authors report no conflicts of interest.

Funding

This work was funded by the National Nuclear Security Administration Office of Environment, Safety, and Health (DOE-NA-ESH).

REFERENCES

(1) Robinson, S. M.; Benker, D. E.; Collins, E. D.; Ezold, J. G.; J. R, G.; Hogle, S. L. Production of Cf-252 and other transplutonium isotopes at Oak Ridge National Laboratory. *Radiochimica Acta* **2020**, *108* (9), 727-746. DOI: 10.1515/ract-2020-0008.

(2) Karay, N. S.; Kyser, E. A.; Pierce, R. A. *Plutonium Purification by Anion Exchange for Mark-18A Target Processing*; SRNL-TR-2017-00193, Rev. 0; Savannah River National Laboratory, 2017.

(3) Kyser, E. A. *Plutonium Loading onto Reillex HPQ Anion Exchange Resin*; WSRC-TR-2000-00372; Westinghouse Savannah River Company, 2001. DOI: 10.2172/773118.

(4) Ryan, J. L.; Wheelwright, E. J. Recovery and Purification of Plutonium by Anion Exchange. *Ind. Eng. Chem.* **1959**, *51*, 60-65. DOI: 10.1021/ie50589a038.

(5) Zhu, Z.-X.; Sasaki, Y.; Suzuki, H.; Suzuki, S.; Kimura, T. Cumulative study on solvent extraction of elements by N,N,N′,N′-tetraoctyl-3-oxapentanediamide (TODGA) from nitric acid into n-dodecane. *Analytica Chimica Acta* **2004**, *527* (2), 163-168. DOI: 10.1016/j.aca.2004.09.023.

(6) McCann, K. P.; Jones, M. A.; Kyser, E. A.; Smith, T. E.; Bridges, N. J. Scaling Trivalent Actinide and Lanthanide Recovery by Diglycolamide Resin from Savannah River Site's Mark-18A Targets. *Industrial & Engineering Chemistry Research* **2021**, *60* (1), 507-513. DOI: 10.1021/acs.iecr.0c03897.

(7) Horwitz, E. P.; McAlister, D. R.; Bond, A. H.; Barrans, R. E. Novel Extraction of Chromatographic Resins Based on Tetraalkyldiglycolamides: Characterization and Potential Applications. *Solvent Extraction and Ion Exchange* **2005**, *23* (3), 319–344. DOI: 10.1081/SEI-200049898.

(8) Nash, K. L. A comparison of new reagents and processes for hydrometallurgical processing of actinides. In Global 2001 international conference on: "back-end of the fuel cycle: from research to solutions", Paris, France; 2001.

(9) Gergoric, M.; Barrier, A.; Retegan, T. Recovery of Rare-Earth Elements from Neodymium Magnet Waste Using Glycolic, Maleic, and Ascorbic Acids Followed by Solvent Extraction. *Journal of Sustainable Metallurgy* **2019**, *5*, 85-96. DOI: 10.1007/s40831-018-0200-6.

(10) Mills, M. S.; Pierce, R. A.; Gibbs, K. M.; Spivey, N. W. Process for the Recovery of Actinide and Lanthanide Oxides vis Thermal Decomposition and Calcination of Loaded Diglycolamide Resin. *Nuclear Technology* **2024**. DOI: 10.1080/00295450.2024.2397206.

(11) Geist, A.; Müllich, U.; Magnusson, D.; Kaden, P.; Modolo, G.; Wilden, A.; Zevaco, T. Actinide(III)/Lanthanide(III) Separation via Selective Aqueous Complexation of Actinides(III) using a

Hydrophilic 2,5-Bis(1,2,4-Triazin-3-YL)-Pyridine in Nitric Acid. *Solvent Extraction and Ion Exchange* **2012**, *30* (5), 433-444. DOI: 10.1080/07366299.2012.671111.
(12) Whittaker, D.; Geist, A.; Modolo, G.; Taylor, R.; Sarsfield, M.; Wilden, A. Applications of Diglycolamide Based Solvent Extraction Processes in Spent Nuclear Fuel Reprocessing, Part 1: TODGA. *Solvent Extraction and Ion Exchange* **2018**, *36* (3), 223-256. DOI: 10.1080/07366299.2018.1464269.
(13) Kyser, E. A. Mills, M. S., Ed.; Personal Communciation.
(14) Lascola, R. J.; O'Rourke, P. E.; Kyser, E. A. A Piecewise Local Partial Least Squares (PLS) Method for the Quantitative Analysis of Plutonium Nitrate Solutions. *Applied Spectroscopy* **2017**, *71* (12), 2579-2594. DOI: 10.1177/0003702817734000.
(15) *DGA Resins*. Eichrom, 2023. https://www.eichrom.com/eichrom/products/dga-resins/ (accessed November 1, 2023).
(16) Tachimori, S.; Sasaki, Y.; Suzuki, S. Modification of TODGA-n-dodecane solvent with a monoamide for high loading of lanthanides(III) and actinides(III). *Solvent Extraction and Ion Exchange* **2002**, *20* (6), 687-699.
(17) Dousma, J.; Bruyn, P. L. D. Hydrolysis-precipitation studies of iron solutions. I. Model for hydrolysis and precipitation from Fe(III) nitrate solution. *Journal of Colloid and Interface Science* **1976**, *56* (3), 527-539. DOI: 10.1016/0021-9797(76)90119-3.
(18) Rodden, C. J. Spectrophotometric determination of praseodymium, neodymium, and samarium. *Journal of Research of the National Bureau of Standards* **1941**, *26*, 557-570.
(19) Rodionova, O. Y.; Tikhomirova, T. I.; Pomerantsev, A. L. Spectrophotometric determination of Rare Earth Elements in aqueous nitric acid solutions for process control. *Analytica Chimica Acta* **2015**, *869*, 59-67. DOI: 10.1016/j.aca.2015.02.037.
(20) Franzen, P.; Gorter, J. P. M. W. C. J. Absorption of light in a solution of samarium nitrate. *Physica* **1943**, *10* (5), 365-368. DOI: 10.1016/S0031-8914(43)90023-0.

Loading Capacity and Dilute Nitric Acid Rinse of Diglocolamide Resin for the Recovery of Transplutonium and Rare Earth Elements from Mark-18A Targets

Matthew S. Mills* and Samuel Uba

Savannah River National Laboratory, Aiken, South Carolina 29898, United States

*Email: Matthew.Mills@srnl.doe.gov

SUPPLEMENTAL INFORMATION

Table S1. Composite effluent cut volumes and compositions.

Element	Cut ID							
	ECA	ECB	ECC	ECD	ECE	ECF	ECG	ECH
	Total volume of column effluent at end of cut (mL)							
	379	755	951	1150	1299	1402	1502	1602
	Total volume of column effluent at end of cut (BV)							
	8.86	17.7	22.2	26.9	30.4	32.8	35.1	37.5
	Concentration (mg/L)							
Cu	2.38E+01	2.59E+01	2.59E+01	2.58E+01	2.57E+01	2.58E+01	2.54E+01	2.55E+01
Fe	2.06E+02	2.76E+02	2.72E+02	2.60E+02	2.61E+02	2.51E+02	2.64E+02	2.54E+02
Sr	2.06E+02	2.76E+02	2.72E+02	2.60E+02	2.61E+02	2.51E+02	2.64E+02	2.54E+02
Y	4.57E+00	5.05E+00	5.03E+00	5.02E+00	5.08E+00	5.09E+00	5.02E+00	5.05E+00
La	< 1.00E-02	< 1.00E-02	< 1.00E-02	< 1.00E-02	< 1.00E-02	< 1.00E-02	< 1.00E-02	< 1.00E-02
Ce	< 1.00E-02	2.08E+01	5.97E+01	5.45E+01	4.40E+01	3.81E+01	3.50E+01	3.31E+01
Pr	< 1.00E-02	3.15E+01	1.29E+02	1.81E+02	1.56E+02	1.39E+02	1.30E+02	1.21E+02
Nd	< 1.00E-02	3.08E+00	1.93E+01	3.96E+01	3.96E+01	3.78E+01	3.66E+01	3.50E+01
Sm	< 1.00E-02	4.31E+00	3.95E+01	1.70E+02	2.41E+02	2.53E+02	2.70E+02	2.71E+02
Eu	< 1.00E-02	1.35E-02	1.95E-01	3.13E+00	1.29E+01	2.57E+01	3.53E+01	4.61E+01
Gd	< 1.00E-02	< 1.00E-02	< 1.00E-02	< 1.00E-02	3.18E-02	8.51E-02	1.38E-01	2.12E-01
Tb	< 1.00E-02	1.44E+00	4.20E+00	3.77E+00	3.10E+00	2.89E+00	2.89E+00	3.07E+00
Dy	< 1.00E-02	1.21E-02	8.99E-02	3.25E-01	4.34E-01	4.63E-01	4.69E-01	4.77E-01
Ho	< 1.00E-02	< 1.00E-02	2.08E-02	9.39E-02	1.41E-01	1.76E-01	1.96E-01	2.14E-01
Er	< 1.00E-02	< 1.00E-02	< 1.00E-02	3.31E-02	4.73E-02	5.38E-02	5.67E-02	5.81E-02
Tm	< 1.00E-02	< 1.00E-02	< 1.00E-02	< 1.00E-02	< 1.00E-02	< 1.00E-02	< 1.00E-02	< 1.00E-02
Yb	< 1.00E-02	< 1.00E-02	< 1.00E-02	< 1.00E-02	< 1.00E-02	< 1.00E-02	< 1.00E-02	< 1.00E-02
Lu	< 1.00E-02	< 1.00E-02	< 1.00E-02	< 1.00E-02	< 1.00E-02	< 1.00E-02	< 1.00E-02	< 1.00E-02

Table S1 (continued). Composite effluent cut volumes and compositions.

Element	Cut ID							
	ECI	ECJ	WC-1	WC-2A	WC-2B	WC-2C	WC-2D	WC-2E
	Total volume of column effluent at end of cut (mL)							
	1702	1812	1898	1925	1951	1978	2004	2030
	Total volume of column effluent at end of cut (BV)							
	39.8	42.4	44.4	45.0	45.6	46.2	46.9	47.5
	Concentration (mg/L)							
Cu	2.53E+01	2.53E+01	1.07E+01	1.53E-01	8.19E-02	3.07E-02	1.32E-02	1.76E-02
Fe	2.54E+02	2.58E+02	9.41E+01	<1.00E-01	<1.00E-01	<1.00E-01	<1.00E-01	<1.00E-01
Sr	2.54E+02	2.58E+02	9.41E+01	<1.00E-01	<1.00E-01	<1.00E-01	<1.00E-01	<1.00E-01
Y	5.06E+00	5.03E+00	1.91E+00	3.27E-02	2.04E-02	< 1.00E-02	< 1.00E-02	< 1.00E-02
La	< 1.00E-02	< 1.00E-02	< 1.00E-02	< 1.00E-02	6.45E-02	1.26E-01	8.53E-02	6.25E-02
Ce	3.17E+01	3.10E+01	1.47E+01	1.46E+00	4.47E-01	2.87E-01	2.18E-01	1.80E-01
Pr	1.12E+02	1.06E+02	5.38E+01	1.90E+01	1.97E+01	2.12E+01	1.43E+01	9.74E+00
Nd	3.33E+01	3.14E+01	1.91E+01	8.00E+00	2.17E+01	2.57E+01	1.56E+01	1.04E+01
Sm	2.72E+02	2.70E+02	1.52E+02	6.54E+01	4.06E+02	4.53E+02	2.54E+02	1.58E+02
Eu	5.91E+01	7.28E+01	5.09E+01	2.31E+01	3.78E+02	3.82E+02	1.81E+02	1.12E+02
Gd	3.21E-01	4.44E-01	3.83E-01	1.73E-01	3.64E+00	4.00E+00	2.02E+00	1.27E+00
Tb	3.48E+00	4.17E+00	3.05E+00	1.11E+00	2.87E+01	3.56E+01	1.95E+01	1.35E+01
Dy	4.71E-01	4.67E-01	2.82E-01	1.23E-01	8.59E-01	1.02E+00	5.90E-01	3.94E-01
Ho	2.33E-01	2.54E-01	1.64E-01	7.30E-02	8.04E-01	8.54E-01	4.46E-01	2.82E-01
Er	5.97E-02	6.16E-02	3.80E-02	1.64E-02	1.32E-01	1.44E-01	7.79E-02	5.05E-02
Tm	< 1.00E-02	< 1.00E-02	< 1.00E-02	< 1.00E-02	4.29E-02	4.38E-02	2.17E-02	1.34E-02
Yb	< 1.00E-02	1.51E-02	1.55E-02	< 1.00E-02	2.18E-01	2.71E-01	1.50E-01	9.52E-02
Lu	< 1.00E-02	< 1.00E-02	< 1.00E-02	< 1.00E-02	< 1.00E-02	< 1.00E-02	< 1.00E-02	< 1.00E-02

- "ECx" represents a feed raffinate cut; "WC-1" represents the 8 M HNO_3 wash; "WC-2x" represents a dilute acid rinse cut.

Spectrometer Details

The spectroscopy system comprises of instruments hardware and a software control system. The hardware system includes:

- Avantes Multichannel Spectrophotometer AVS-RACKMOUNT-USB2
- Avantes spectrophotometer: AS60014U21, AS60015U21
- Optical beam combiner/splitter BSC-DA-SRNL1
- Xenon arc lamp AVALIGHT-XE-HP
- Tungsten-Halogen lamp AVALIGHT-HAL
- Fiber optic cables – Multimode fibers, 400 μm high-OH core, 0.22 na
- Computer with USB Interface
- COTS assembled 90mm Stainless steel flow cell. Swagelok #SS-2000-3
- COTS collimator, Edmund Optics #88-173

The instrument control software system is a control program written in the Visual Basic environment.

- Hardware interface program VB_App_AS7010.EXE
  - *To configure and communicate with Avantes spectrophotometers*.
- Spectroscopic data processing and analysis program Avantes_Model_E.XLSM workbook
  - *Convert raw intensity signals to corrected spectra and other useful materials characteristics*.